Journal of Soil Sciences and Agricultural Engineering

Journal homepage & Available online at: www.jssae.journals.ekb.eg

Optimization and Sensitivity Analysis of Standalone PV-Wind-Biomass-Battery Hybrid Systems for Sustainable Agricultural Electrification in Remote Areas

Jado, A.¹*; Tatiana Morosuk² and Jinming Pan³

- ¹ Mansoura University, Department of Agricultural Engineering, Mansoura 35516, Egypt.
- ²Institute for Energy Engineering, Technical University of Berlin, Berlin 10587, Germany.
- ³Zhejiang University, Department of Biosystems Engineering, Hangzhou 310058, China.







This study examines the techno-economic feasibility of hybrid energy systems that utilize renewable sources to meet the electrical demands of a livestock and poultry farm in the New Valley Governorate of Egypt. In this study, HOMER Pro was used to explore different hybrid energy system setups that include solar panels, wind turbines, biomass generators, and battery storage. The simulations were based on accurate local weather data and real hourly electricity demand at the site. The photovoltaic/wind/biomass/battery system was the greatest economical option, with a net present cost (NPC) of 9.62 million USD and a levelized cost of energy (LCOE) of 0.716 USD/kWh. Solar energy provided the majority of the farm's electricity (82%), while wind and biomass made smaller but important contributions. Sensitivity analyses showed that even modest improvements, like reducing capital costs or slightly increasing renewable resource availability, could make these systems even more affordable. The findings highlight how thoughtful combinations of renewable sources can offer reliable, sustainable, and practical energy solutions for agriculture in remote areas.

Keywords: Renewable Power System, HOMER Pro Simulation, Microgrid Design, Rural Electrification, Economic Optimization

INTRODUCTION

The increasing demand for clean, reliable, and decentralized energy solutions has accelerated interest in isolated microgrids, particularly for rural and remote communities. Isolated microgrids have become a key solution for delivering sustainable and reliable energy, especially in areas lacking access to centralized grids (Yadav *et al.*, 2024).

The incorporation of energy from renewable sources such as solar photovoltaic, wind turbines, hydroelectric generators, and energy storage systems into microgrids allows enhanced efficiency and less dependence on fossil fuels (Belrzaeg et al., 2023). This setup enables the utilization of local resources, balancing energy supply and demand effectively (Alzahrani et al., 2023). Microgrids enhance system reliability by operating independently during main grid outages, providing uninterrupted electricity to connected consumers (Quizhpe et al., 2024). This capability is very beneficial in remote locations and essential facilities. (Saxena et al., 2024). The strategic coordination and management of these diverse energy resources are crucial for achieving operational efficiency, sustainability, and resilience. This integration is supported by advanced optimization techniques and energy management systems that dynamically adjust energy generation and distribution in response to real-time conditions (Dixit, 2024).

Many hybrid renewable energy systems have been explored in recent research, bringing together different

renewable sources to improve energy reliability and lessen the reliance on traditional fossil fuels. Different hybrid renewable energy configurations have been widely explored for their ability to optimize energy production in off-grid and rural areas. These include systems that combine photovoltaic panels with wind turbines (Won et al., 2017; Zhang et al., 2019), wind turbines with biomass (Osmani & Zhang, 2014), photovoltaic panels with biomass (El-Sattar et al., 2022; Tiam Kapen et al., 2022), and more integrated setups that bring together photovoltaic panels, wind turbines, and biomass sources (Mahdavi et al., 2023). Alongside these generation sources, various energy storage technologies, particularly battery energy storage systems, have been explored to improve system stability and ensure continuous power supply. Other storage methods, such as Supercapacitor-Battery combinations (Kotb et al., 2022; Lin & Lei, 2017), Flywheel-Battery systems (Barelli et al., 2019; Ngila & Farzaneh, 2023), and Pumped-Hydro Storage (PHS) with batteries (Das et al., 2019; Guezgouz et al., 2019), have also been investigated for their role in enhancing microgrid performance.

Jahangir *et al.* (2024) utilized HOMER software to model and optimize a hybrid renewable energy system. Their work involved simulating different configurations that combined wave energy converters, wind turbines, photovoltaic panels, biogas generators, and lithium-ion batteries, ultimately achieving a cost-effective and reliable power supply for remote villages. HOMER proved to be a valuable tool for assessing both the economic and technical

* Corresponding author. E-mail address: Jado@mans.edu.eg DOI: 10.21608/jssae.2025.379482.1283 feasibility of such complex systems. El-Sattar *et al.* (2021) proposed an optimal hybrid renewable energy system combining photovoltaic panels, wind turbines, biomass, and battery storage to enhance rural electrification in Abu-Monqar, Egypt. Among the three configurations evaluated, the system integrating biomass with wind turbines and batteries, optimized using the Slime Mould Algorithm (SMA), achieved the best performance, with NPC of approximately 3.48 × 10⁶ USD, an energy cost (EC) of 0.119 USD/kWh, and a loss of power supply probability (LPSP) of 3.25%. The use of HOMER software allows for the optimization of hybrid systems by evaluating different configurations to minimize the NPC and COE (El-Maaroufi *et al.*, 2024).

The existing literature on hybrid renewable energy systems has mainly concentrated on optimizing system design by minimizing either the levelized cost of energy or the net present cost. However, most sensitivity analyses have been limited to a narrow set of parameters, often overlooking critical factors such as project lifetime, seasonal load variations, and the dynamic behavior of storage systems. Furthermore, while several studies have addressed the integration of energy storage systems into hybrid configurations, the impact of storage performance on overall system cost and reliability remains insufficiently explored. One of the key challenges facing isolated microgrids with a high penetration of renewable energy sources is the management of excess energy generation and unmet load, which can significantly affect both system economics and operational stability (Emrani & Berrada, 2024).

This study aims to conduct a techno-economic feasibility analysis and optimal design of a hybrid renewable energy system combining photovoltaic panels, wind turbines, a biomass generator, and battery energy storage for rural electrification. The proposed system is designed to meet the energy demands of a poultry and livestock farm located in the New Valley Governorate of Egypt. Through detailed simulation, optimization, and sensitivity analysis using HOMER software, the study seeks to minimize the net present cost and the cost of energy while ensuring reliable and sustainable energy supply under varying operating conditions.

MATERIALS AND METHODS

In this paper, simulations, optimizations, and sensitivity analyses for an integrated renewable energy system using meteorological data along with the load demand particular to the case study area from the New Valley Governorate of Egypt are accomplished by means of HOMER software. The study area is a 2000-feddan agricultural zone situated in the New Valley Governorate, Egypt. The site comprises an integrated farming system that includes a livestock farm, a poultry farm, and cultivated areas with date palms, wheat, and corn (maize). These agricultural activities generate a significant volume of organic residues, which are considered the primary source of biomass used in the proposed hybrid energy system.

Simulation and optimization using HOMER software

HOMER software enables the simulation and configuration of energy sources, energy storage systems (ESS), electrical loads, converters, and optimization tools tailored to the characteristics of the site and user preferences.

The microgrid design optimization process aims to minimize the objective function while ensuring compliance with reliability requirements (Siddaraju et al., 2022). It evaluates and ranks possible system configurations Depending on the lowest net NPC and COE. Figure 1 illustrates the structure for the development and performance evaluation of standalone microgrids. Wind and solar energy resources are available in the New Valley Governorate, Egypt, which was selected as the research site. Site is geographically located at 24°32.7'N latitude and 27°10.4'E longitude. Site-specific meteorological data, including the speed of the wind, ambient temperature, and sun irradiance, were obtained from the HOMER software database. Figure 2 illustrates the monthly average values of speed of the wind, temperature, radiation from the sun, and clearness index.

The chosen site benefits from consistent access to wind, biomass, and solar energy resources throughout the year. The proposed renewable energy system primarily consists of a biomass generator, a turbine for wind power, a battery bank, a converter, and a source of electricity with an average consumption of 2846.3 kWh/day. This study aims to design a cost-effective and sustainable power system able to fulfill the energy demands of a poultry farm as well as livestock production. To identify the most economically viable renewable energy source, this paper evaluates four different renewable energy configurations, which include Photovoltaic-biomass-wind-batteries, photovoltaic-batteries-wind, photovoltaic-biomass-batteries, and photovoltaic-batteries, as illustrated in Fig. 3.

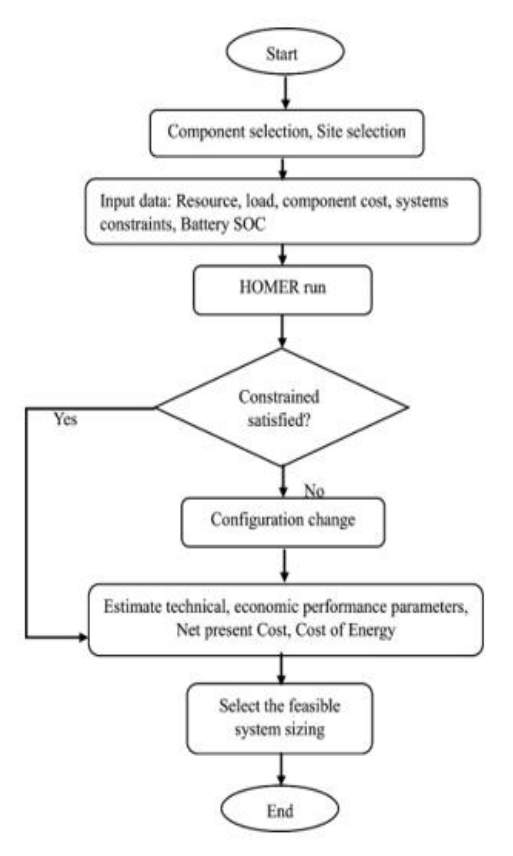


Fig. 1. HOMER software optimization flow for hybrid systems (Das *et al.*, 2024) .

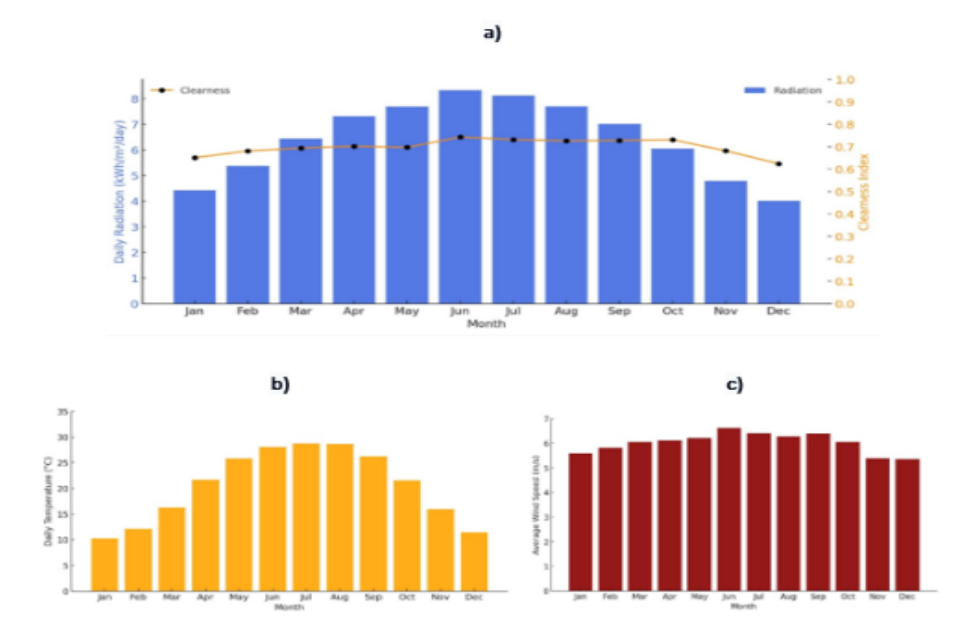


Fig. 2. Climate data: a) Solar irradiance, b) Ambient temperature, and c) Wind speed

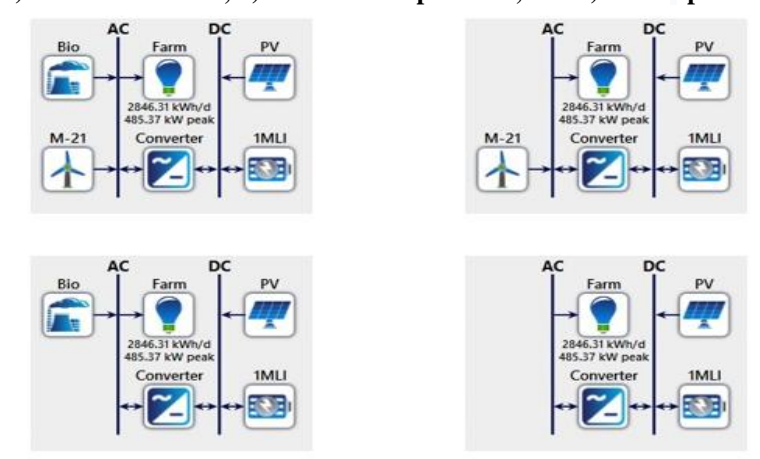


Fig. 3. Schematic representation of different hybrid renewable energy system

The region under examination has a mean load of roughly 2846.3 kWh per day, a peak load of 485.37 kW, and a load factor of 0.24. As shown in Figure 4, the load demand with perturbation factors.

is illustrated, presenting: (a) a profile of the daily load, (b) the profile of monthly load, and (c) the annual profile of loads with perturbation factors.

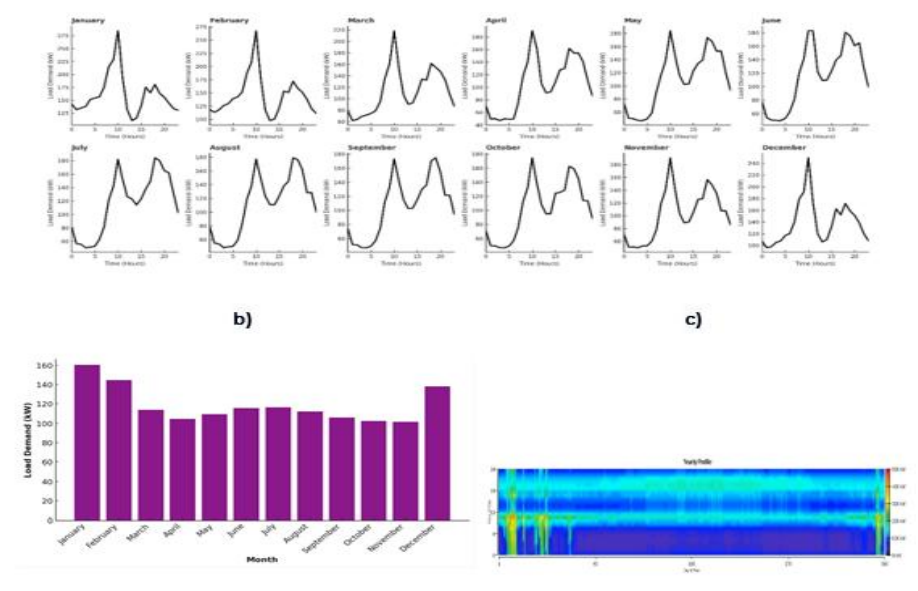


Fig. 4. Load demand, a) daily, b) monthly, and c) load profile for the year

The load demand analysis highlights significant seasonal and daily variations in electricity consumption at the farm. The highest energy demand occurs in winter (January, February, and December) due to increased heating requirements, whereas lower consumption is observed in warmer months when heating is unnecessary. There are two peaks in the hourly load profile, one between 5:00 and 10:00 AM and another between 6:00 and 10:00 PM. These peaks correspond to critical farm operations including feeding, lighting, and ventilation. In contrast, late-night hours (0.00 - 4.00 AM) exhibit minimal energy usage, reflecting reduced farm activity. The winter months show higher and sustained peak loads, while in summer, the demand is lower and more stable. Understanding these patterns is crucial for optimizing energy efficiency and integrating renewable energy sources to ensure a reliable and cost-effective power supply throughout the year.

Analytical modeling of hybrid microgrid components Solar PV generation

The quantity of electrical energy generated by solar photovoltaic panels is primarily influenced by solar irradiance, as estimated by the HOMER software. The electricity generated from the photovoltaic panels, denoted as $P_{S,pv}(t)$, is calculated using the following expression (Kumar et al., 2022):

$$P_{S,pv}(t) = P_{Rt,pv} \times d_{loss,pv} \times \left(\frac{l_h(t)}{l_{STC}}\right) \times [1 + \alpha_{T,pv}(T_c - T_{STC})]$$
 (I)
Here, $d_{loss,pv}$ is the derating factor for the photovoltaic

system, I_h (t) is the sun irradiance every hour, I_{STC} is the irradiance under conventional testing conditions, $\alpha_{T,pv}$ is the temperature coefficient, T_c is the Photovoltaic cell temperature, T_{STC} is the cell temperature under conventional testing conditions, and $P_{Rt,pv}$ is the nominal power output of the photovoltaic panel.

During night ime, the PV cell temperature T_c is approximately equal to the ambient temperature T_a , but during the daytime, T_c can exceed T_a by around 30 °C or more. The temperature of the PV cell is determined by the equation (Kumar et al., 2022):

$$T_c(t) = T_a(t) + T_{c.Noct} - T_{a.Noct} \times \left(\frac{I_h(t)}{I_{T.Noct}}\right) \times \left(1 - \frac{\mu_{mp}}{\zeta \varphi}\right) (2)$$
In this formula, $T_{a.Noct}$ is the ambient temperature

(NOCT), $T_{c,Noct}$ is the NOCT of the Photovoltaic cell, $I_{T,Noct}$ is the solar irradiance at NOCT conditions, μ_{mp} is the efficiency of the PV panel at the maximum power point, ζ is the solar transmittance, and φ is the PV array's solar absorptance. The technical as well as economical specifications of the solar photovoltaic model utilized in the analysis are derived from Yadav et al. (2024).

Wind power system

HOMER software estimates wind turbine power output using a three-step process at each simulation time step. First, it extrapolates the wind speed to the turbine's hub height based on site-specific conditions. Then, it determines the theoretical power output using the turbine's power curve in relation to the calculated wind speed and standard air density. Finally, the output is corrected to account for the actual air density at the given location, ensuring a more accurate representation of real-world performance.

The wind speed at the turbine hub height is determined using input parameters specified in the Wind Resource and Wind Shear sections. When a logarithmic wind profile is applied, the hub-height wind velocity V_h calculated using the following equation (Youssef et al., 2023):

$$V_h = V_a \times \frac{\ln(\frac{Z_h}{Z_s})}{\ln(\frac{Z_a}{Z_s})}$$
 (3)

Where:

 V_h Hub-height wind speed (m/s)

 Z_s Roughness length of the surface (m)

 V_a Anemometer-height wind speed (m/s)

Z_a Anemometer installation height (m)

 Z_h Height of turbine hub (m)

If the power law is employed, wind speed is calculated using (Youssef et al., 2023):

$$V_h = V_a \times [\ln(Z_h/Z_a)]^Y$$
 (4) Where Y is the power law exponent.

Once the wind speed at the rotor hub level is established, HOMER utilizes the turbine's power curve to estimate its output. Since power curves assume STP conditions, the actual power output is corrected by the air density ratio, as shown below (Youssef et al., 2023):

$$P_W = P_n \times (\rho_a/\rho_n) (5)$$

Where:

Pw Actual power output, kW

Power at standard conditions, kW

Turbine hub height, kg m³

Standard air density

In this study, the wind turbine is modeled with a hub height of 31.8 meters, a rated capacity of 100 kW, and a rotor radius of 10.5 meters. Monthly average wind speed data for the selected site were sourced from the NASA meteorological database, indicating an annual mean wind speed of 6.03 m/s. As shown in Figure 5, the highest wind speeds occur in June, while the lowest values are observed in December. The technical and economic specifications of the wind turbine used in this analysis are based on data provided by Yadav et al. (2024).

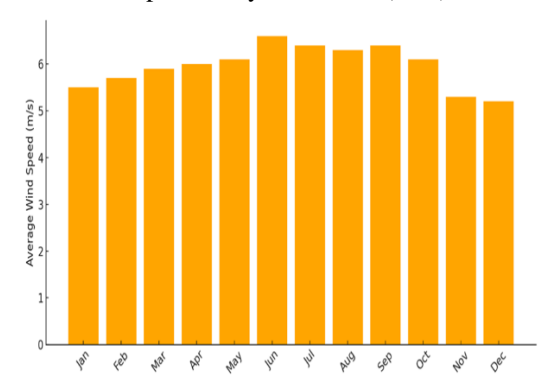


Fig. 5. Average monthly wind speed profile for the study area

Biomass power generation systems

Electricity generation from biomass can occur through biochemical pathways, such as anaerobic digestion and fermentation, or through thermochemical processes, including gasification, pyrolysis, and direct combustion. These methods convert biomass into gaseous or liquid fuels suitable for energy production (Youssef et al., 2023). This study focuses on utilizing agricultural crop residues available in Egypt as a biomass source. The average monthly availability of biomass at the selected site is illustrated in Fig. 6, with an average of approximately 2.43 tons per day. Peak biomass availability occurs during the months of January and February. The required biomass quantity is collected from agricultural residues locally available in the study area, primarily from date palm fronds, wheat straw, and corn stalks.

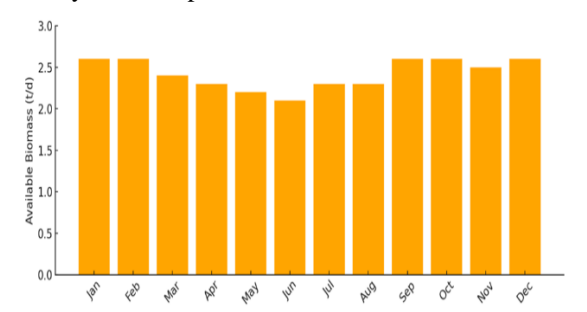


Fig. 6. The average monthly availability of biomass at the selected site

In this study, a biogas generator with an auto-sized configuration and a rated capacity of 500 kW is considered. The capital investment for the biomass-based generation system is assumed to be \$3000 per kilowatt, while the replacement cost is estimated at \$1250 per kilowatt. Furthermore, the operation and maintenance cost is set at \$0.10 per operating hour per kilowatt, reflecting standard industry assumptions. The biomass engine has an operating

Table 1. Specifications of the Battery Storage System

lifetime of 20,000 hours. The system employs a gasifier engine to convert solid biomass into gas with high efficiency, which is then used in internal combustion (IC) engines for power generation.

The biomass generator output power, denoted as $P_b(t)$, is calculated using the following equation (Eteiba et al., 2018):

$$P_{b}(t) = \left(\frac{N_{g}}{F}\right) \left[\frac{\eta_{g} \times H_{W} \times B(t)}{H_{g}} - F_{n} P_{g}\right] (6)$$

Where:

 P_b Biomass-based power generation (kW)

 \mathbf{F}_n No-load fuel consumption (kg/h/kW)

F Low specific fuel consumption (kg/h/kW) H_g

Low heating value of producer gas (MJ/kg)

 H_W Low heating value of wood (MJ/kg)

B Biomass feed rate (kg/h)

 $N_{\rm g}$ Number of generators

Gas efficiency

 η_g P_g Generator rated capacity (kW)

Modeling of the battery bank system

Batteries are essential components of hybrid energy systems, functioning as storage units for excess energy produced by renewable sources, which can subsequently be utilized to satisfy load demand. The specifications of the batteries utilized in the hybrid system are outlined in Table 1.

Those It specimentions of the Butter j Storage Sjotem					
Battery Specification	Value	Battery Specification	Value		
Nominal electric potential (V)	600V	Nominal energy (kWh)	1000 kWh		
Nominal capacity (Ah)	1670Ah	Roundtrip efficiency (%)	90%		
Maximum charging current (A)	1670A	Maximum discharging current (A)	5000 A		
The first phase of charge (%)	100%	Minimal level of charge (%)	20%		
Lifetime (years)	15 years	Throughput (kWh)	3000000 kWh		

RESULTS AND DISCUSSION

Hybrid system optimization results

Table 2 presents the optimization outcomes for various hybrid energy system configurations. It outlines the rated capacities (in kW) of individual system components and indicates the number of lithium-ion batteries used in each setup. The table also includes key economic indicators, such as the net present cost, levelized cost of energy, annual operating cost, and initial capital investment. Among the evaluated configurations, the PV/Wind/Biomass/Batteries system exhibits the most favorable economic performance. It requires the fewest batteries and achieves the lowest values across all economic metrics, including NPC, LCOE, annual operating cost, and upfront capital cost. The optimal configuration results in an NPC of 9.62 million USD and an LCOE of 0.716 USD/kWh.

Table 2. Optimization results for different configurations of hybrid energy systems (based on a 25-year project lifetime)

System	PV	Wind	Biomass	No. of Lithium-Ion	Converter	NPC	LCOE	Operating	Initial Capital
Configuration	(kW)	Turbine(kW)	(kW)	Batteries (1MWh)	(kW)	(\$)	(\$)	Cost (\$/yr)	Cost (\$)
PV/Wind/Biomass/Batteries	1409	100	500	5	541	9.62 M	0.716	120,374	8.06 M
PV/Wind/Batteries	1401	100	-	8	623	10.9 M	0.811	171,499	8.67 M
PV/Biomass/Batteries	2647	-	500	5	681	12.2 M	0.910	133,139	10.5 M
PV/Batteries	2529	-	-	8	568	13.2 M	0.982	182,155	10.8 M

Figure 7 illustrates the comparison of NPC and LCOE for four hybrid energy system configurations.

Among all systems, the PV/Wind/Biomass/Batteries configuration demonstrates the lowest NPC (9.62 million USD) and lowest LCOE (0.716 USD/kWh), indicating superior cost-effectiveness. In contrast, the PV/Batteries-only system shows the highest NPC (13.2 million USD) and highest LCOE (0.982 USD/kWh), making it the least economical option. The inclusion of both wind and biomass significantly components reduces long-term costs, confirming the economic advantage of integrating multiple renewable sources with energy storage.

Table 3 presents the cost breakdown of the optimal PV-wind-biomass hybrid energy system equipped with lithium-ion batteries. It details the capital cost, replacement cost, operating cost, salvage value, and resource cost for each system component. Additionally, the table summarizes the

total cost of each component and provides the overall NPC of the entire hybrid system.

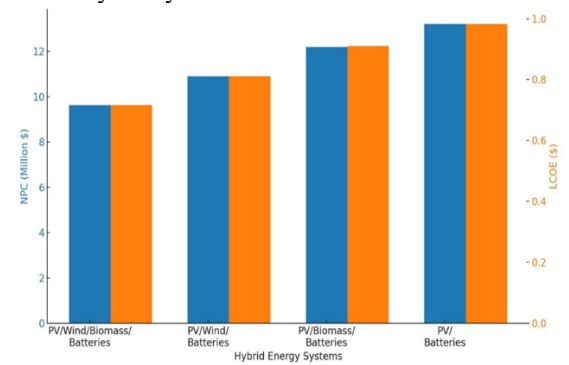


Fig. 7. Net Present Cost and and levelized cost comparison for various hybrid energy systems

Table 3. Cost distribution of components in the optimal PV-wind-biomass hybrid system

Component	Capital Cost (USD)	Replacement Cost (USD)	O&M (USD)	Salvage (USD)	Total (USD)
Generic 1MWh Li-Ion	\$3.5 M	\$742,479	\$646,375	\$139,742	\$4.75 M
Biogas generator	\$1.5 M	\$35,438	\$56,390	\$14,912	\$1.59 M
Flat plate PV	\$2.8 M	\$0.00	\$182,162	\$0.00	\$3 M
Converter	\$162,167	\$34,401	\$0.00	\$6,474	\$190,093
XANT M-21 [100kW]	\$80,000	\$0.00	\$5,171	\$0.00	\$85,171
System Total	\$8.06 M	\$812,319	\$904,940	\$161,129	\$9.62 M

Figure 8 illustrates the detailed cost distribution of each component within the optimal hybrid energy system. As shown, the flat plate PV system accounts for the highest capital cost. The 1 MWh lithium-ion batteries contribute the most to the operating, replacement, and salvage costs.

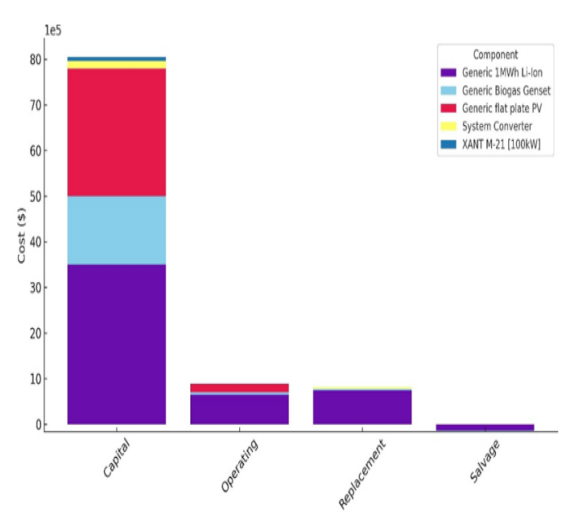


Fig. 8. Capital, replacement, operating, and salvage costs of System components in the optimal hybrid energy configuration

Table 4 presents a summary of the energy output from each component of the optimized PV—wind—biomass hybrid power system. Among the three sources, the solar photovoltaic (PV) system contributed the highest share, accounting for approximately 82% of the total electricity generated. Wind turbines produced around 9.8%, while the biomass unit contributed the smallest portion, generating about 8.2% of the total output. Additionally, the system produced 68.2% more electricity than the load demand, indicating a significant surplus. Figure 9 illustrates the monthly electricity generation profile of the hybrid system. As indicated, the highest electricity production occurs in August, whereas December marks the lowest energy generation throughout the year.

Fig. 10 illustrates the biomass generator's power output over a 24-hour period across the year for the optimized hybrid energy system. The electrical output ranges from a minimum of 250 kW to a maximum of 500 kW, with a mean electrical output of 256 kW. The annual electricity production from the biogas genset is 282,206 kWh/year. The system consumes 885 tons of biomass per year, resulting in a specific fuel consumption of 2.20 kg/kWh, and an overall fuel energy input of 946,476 kWh/year. The mean electrical efficiency is reported as 29.8%. Operational parameters indicate a total of 1,102 hours of operation per year, 515 starts/year, and an operational life expectancy of 18.1 years. The capacity factor is 6.44%, with a fixed generation cost of \$10.0/hour, and zero marginal generation cost.

Table 4. Summarizes the production of each component in the ideal photovoltaic-wind-biomass system.

Production	Yearly Energy	Contribution	
Troduction	Output (kWh/yr)	(%)	
Generic Biogas Genset	282,206	8.2%	
Generic flat plate PV	2,823,744	82%	
XANT M-21 [100kW]	337,624	9.8%	
Total	3,443,574	100%	
Excess Electricity	2,347,518	68.2%	

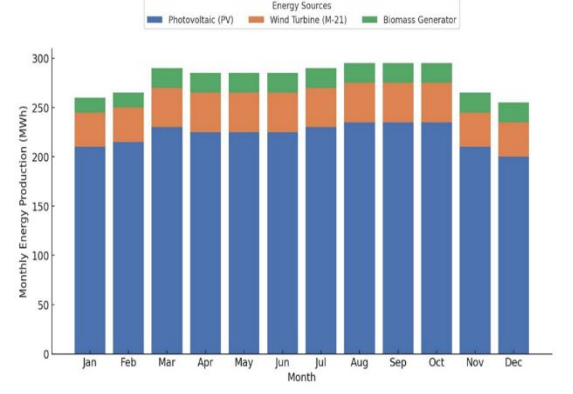


Fig. 9. Monthly power generation profile of the ideal hybrid energy system

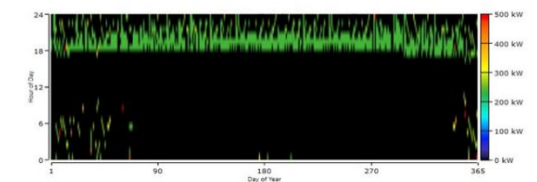


Fig. 10. Biomass generator power profile.

Figure 11 presents the annual power output profile of the photovoltaic system, illustrating its 24-hour generation pattern across all days of the year for the optimal hybrid energy configuration. The maximum output power recorded is 1,388 kW, while the average output power is 322 kW. The PV system produces a mean daily energy output of 7,736 kWh/day, resulting in a total annual production of 2,823,744 kWh/year. It operates for approximately 4,368 hours per year, achieving a capacity factor of 22.9%. The LCOE is 0.0822 \$/kWh, and the system exhibits a PV penetration rate of 272%, indicating its significant contribution to the overall hybrid energy system.

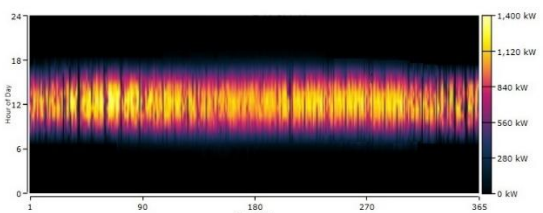


Fig. 11. Photovoltaic power generation pattern.

Figure 12 presents the annual power output profile of the wind turbine in the optimal hybrid power system, showing its variation over a 24-hour cycle throughout the year. The wind subsystem has a total rated capacity of 100 kW, with a maximum output of 100 kW and an average output of 38.5 kW. The system operates for approximately 7,569 hours per year, delivering a total annual energy production of 337,624 kWh/year. The capacity factor is 38.5%, reflecting consistent utilization across the year. The wind penetration into the overall system is 32.5%, and the LCOE for wind generation is 0.0195 \$/kWh.

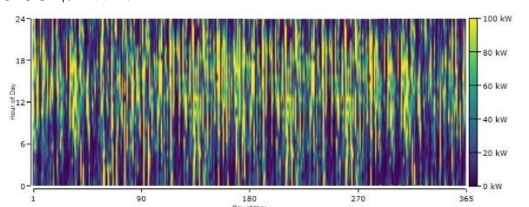


Fig. 12. Annual wind turbine power profile

Figure 13 shows the daily and seasonal variation in the state of charge (SOC) of lithium-ion batteries throughout the year in the optimal hybrid energy system. The SOC ranges from a minimum of approximately 20% to a maximum of 100%, indicating controlled charge/discharge behavior throughout the year. The battery bank consists of 5 lithium-ion units, each rated at 1 MWh, arranged in 5 parallel strings with a bus voltage of 600 V. The total nominal capacity is 5,000 kWh, with 4,000 kWh usable. The batteries deliver an annual energy input of 260,626 kWh/year and output of 235,087 kWh/year, resulting in energy losses of 26,091 kWh/year and minor storage depletion of 552 kWh/year. The annual energy throughput is 247,803 kWh/year. The system exhibits 33.7 hours of autonomy and is expected to last 15 years, with a lifetime throughput of 3,717,046 kWh.

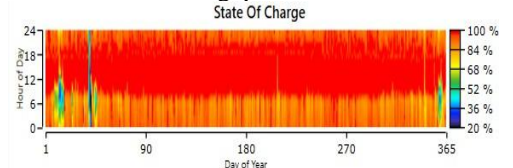


Fig. 13. Yearly battery SOC pattern

Sensitivity analysis

Sensitivity analysis serves as a crucial approach for examining how a system responds to changes or uncertainties in input parameters. In this study, it is applied with a focus on techno-economic aspects to understand how key factors impact the net present cost and the levelized cost of electricity. The variables analyzed include the discount rate, inflation rate, project lifetime, capital cost, wind speed, solar irradiance, and the allowable capacity shortage.

Sensitivity of economic indicators to capacity shortage levels

Figure 14 shows the sensitivity analysis of the NPC and the COE with respect to varying capacity shortage percentages ranging from 0% to 10%. It is evident that both NPC and COE decrease consistently as the allowed capacity shortage increases. At 0% capacity shortage, where the system is designed to fully meet the load at all times, the NPC and COE are at their maximum values of approximately \$11.2 million and 0.71 \$/kWh, respectively. As the capacity shortage increases to 2%, 4%, 6%, 8%, and 10%, the NPC declines steadily to a minimum of \$4.1 million, and the COE decreases to 0.24 \$/kWh. This trend highlights the economic

benefit of relaxing the reliability requirement, as it allows for downsizing system components and reducing overcapacity. The reduction in NPC and COE from 0% to 10% is approximately 63.39% and 66.2%, respectively.

Figure 15 illustrates the relationship between predefined capacity shortage limits and the resulting changes in both capacity shortage and excess energy generation. As expected, the obtained shortage percentage increases proportionally, reflecting a relaxation in system reliability constraints. Simultaneously, the percentage of excess energy generation shows a marked decline from approximately 25–26% at 0–4% capacity shortage to around 10% at 10% shortage. This decline suggests that systems designed under tighter reliability constraints tend to be oversized, resulting in a higher amount of surplus electricity.

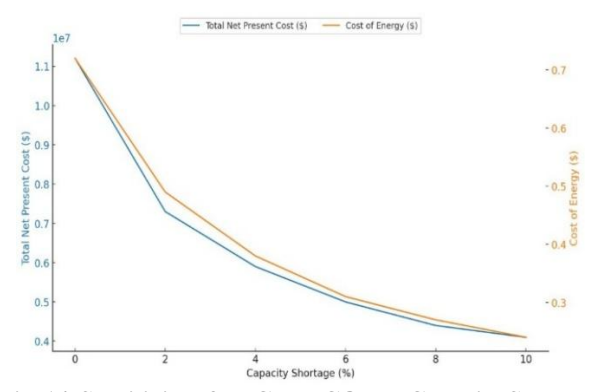


Fig. 14. Sensitivity of NPC and COE to Capacity Shortage Levels.

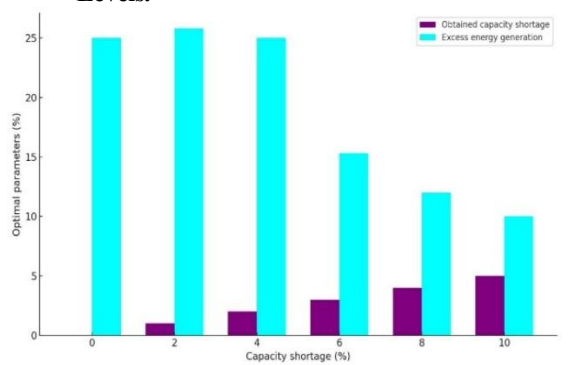


Fig. 15. Impact of capacity shortage on reliability and excess generation.

Effect of capital cost variation on economic performance

Figure 16 depicts the impact of capital cost variations on the economic performance of the optimal hybrid renewable energy system.

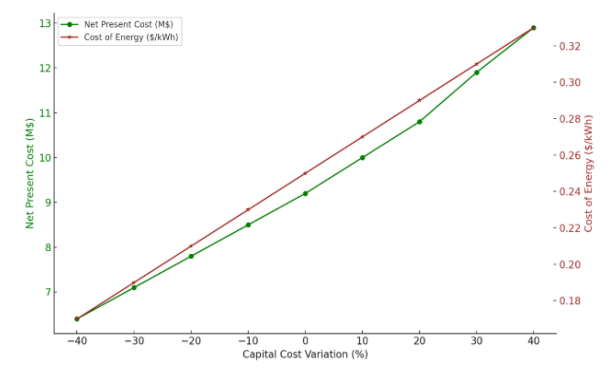


Fig. 16. Sensitivity of NPC and COE to Capital Cost Variation

As observed, both the NPC and COE exhibit a nearly linear increase with rising capital costs. When capital cost is reduced by 40%, the system achieves the lowest NPC and COE, approximately \$6.4 million and \$0.17/kWh, respectively. Conversely, a 40% increase in capital cost results in the highest values, with NPC reaching nearly \$12.9 million and COE around \$0.33/kWh. These results emphasize the strong dependency of system economics on capital investment, highlighting the importance of cost-efficient component selection and market price trends in optimizing hybrid renewable energy systems.

Effect of project lifetime on economic performance

Figure 17 illustrates the impact of extending the project lifetime from 20 to 30 years on the total Net Present Cost and the Levelized Cost of Electricity (COE) for the optimal hybrid energy system. The results show that as the project lifetime increases, the NPC gradually rises from approximately \$9.25 million at 20 years to around \$9.9 million at 30 years. This increase is attributed to the accumulation of operational and maintenance costs over a longer time horizon.

Conversely, the COE decreases steadily from about \$0.775/kWh to approximately \$0.665/kWh as the project duration extends. This reduction in COE is due to the fixed capital investment being spread over a longer operational period and greater total energy production.

These findings highlight a key trade-off in system planning: while longer project durations lead to higher cumulative costs, they play a key role in enhancing the system's economic efficiency by lowering the cost per unit of energy.

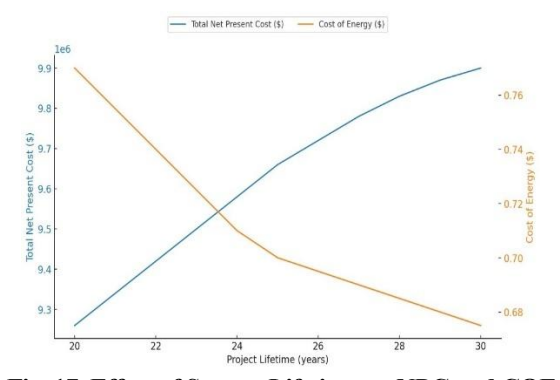


Fig. 17. Effect of System Lifetime on NPC and COE

Effect of solar irradiation on economic performance

The sensitivity analysis investigates the effect of varying solar irradiation on the techno-economic performance of the optimal hybrid energy system. The base case average solar irradiation is 6.44 kWh/m²/day, and it is increased progressively up to 7.2 kWh/m²/day (an increase of approximately 11.78%). As shown in Fig. 18, both the NPC and the COE exhibit a declining trend with the increase in solar irradiation. Specifically, the NPC decreases from approximately \$9.63 million at 6.44 kWh/m²/day to around \$9.01 million at 7.2 kWh/m²/day, indicating a reduction of about 6.44%. A similar trend is observed in the COE, which declines from \$0.715/kWh to \$0.685/kWh, corresponding to a reduction of about 4.2%. This inverse relationship reflects that higher solar availability improves the performance of the PV

subsystem, reduces reliance on other costly generation sources, and leads to a more cost-effective system configuration.

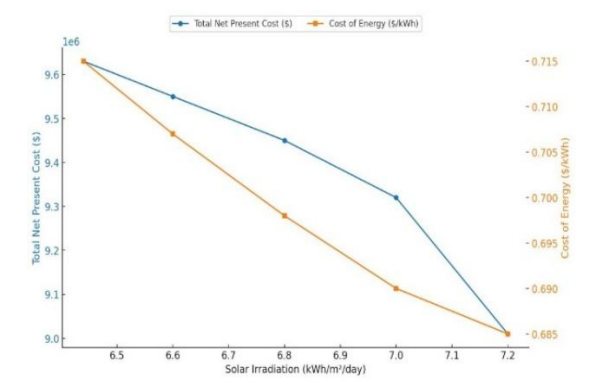


Fig. 18. Variation in NPC and COE as a Function of Solar Irradiance

Effect of wind speed variation on economic performance

Wind speed, being inherently variable, was treated as an uncertain parameter and included in the sensitivity analysis. The baseline average annual wind speed at the study site is $6.03 \, \text{m/s}$. To evaluate its effect on the techno-economic performance of the system, the wind speed was progressively increased up to $7.0 \, \text{m/s}$. Figure 19 presents the impact of increasing wind speed on the Net Present Cost and Levelized Cost of Electricity.

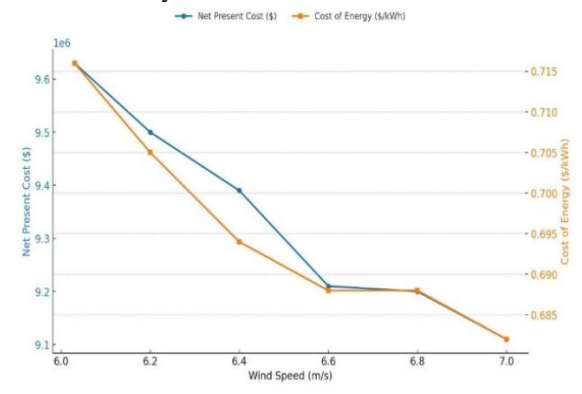


Fig. 19. Sensitivity of NPC and LCOE to Wind Speed Variation

The analysis reveals that higher wind speeds contribute to improved economic performance, as both NPC and COE decline with increased wind availability. When the average wind speed increases from 6.03 m/s to 7.0 m/s—a 16% rise—the NPC decreases from approximately \$9.63 million to \$9.11 million, while the COE drops from \$0.716/kWh to \$0.682/kWh.This trend indicates an improvement in the overall economic performance of the system with enhanced wind availability. However, the decline in both NPC and COE is not entirely uniform. Between wind speeds of 6.4 m/s and 6.6 m/s, both indicators show minimal change, and the curves flatten, suggesting diminishing marginal returns at higher wind speeds. This behavior can be attributed to system design limitations or the saturation of wind turbine output at those levels. In summary, the analysis confirms that higher wind speeds can enhance the costeffectiveness of the hybrid energy system, though the benefits tend to stabilize beyond a certain threshold. Effect of discount and inflation rates on economic performance

The discount rate and inflation rate are crucial financial factors that can greatly affect the economic viability and overall performance of a hybrid energy system. In this

study, a sensitivity analysis was carried out to evaluate how changes in these parameters influence system economics. The discount rate was adjusted between 8% and 11% to observe its effect on both the NPC and the COE. Figure 20(a) shows that increasing the discount rate leads to a noticeable decline in the NPC, while the COE shows a moderate rise. When the discount rate increases from 8% to 11%, the NPC drops from approximately \$9.63 million to \$9.01 million, reflecting a 6.4% reduction. Meanwhile, the COE increases from \$0.88/kWh to \$0.92/kWh, indicating a rise of about 4.5%. Similarly, the inflation rate was varied from 2% to 4% to observe its influence. As shown in Fig. 20(b), an increase in the inflation rate results in a higher Net Present Cost and a lower Cost of Electricity (COE). When the inflation rate rises from 2% to 4%, the NPC increases from approximately \$9.62 million to just over \$10 million, representing a growth of about 4.1%. In contrast, the COE declines from around \$0.715/kWh to \$0.6/kWh, marking a reduction of nearly 16%. These results emphasize the importance of accurately forecasting economic parameters, as they play a crucial role in long-term financial planning and viability of integrated renewable energy setups.

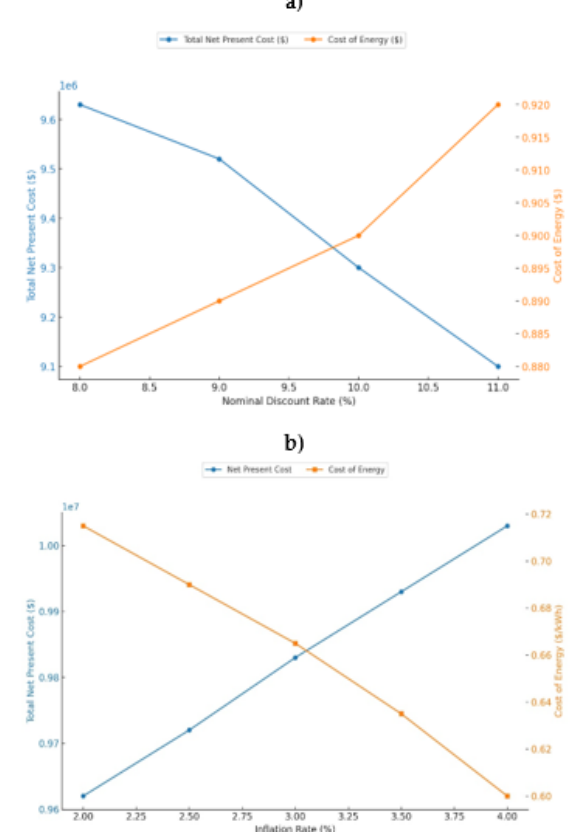


Fig. 20. Sensitivity of NPC and LCOE to (a) Discount Rate and (b) Inflation Rate

Model Validation through Comparative Analysis

To verify the reliability of the simulation outcomes, a comparative analysis was conducted with the study by Youssef *et al.* (2023), which modeled a similar hybrid PV-Wind-Biomass-Battery system in Egypt's New Administrative Capital. While both studies used comparable modeling methods and battery configurations, the present study addressed a significantly higher energy demand (2737 kWh/day vs. 2656 kWh/day) and peak load (2846 kW vs. 371.8 kW). These differences led to increased biomass use (885 vs. 216 tons/year) and a higher rate of excess electricity

(68.2% vs. 26.8%), contributing to a higher LCOE (0.716 vs. 0.382 USD/kWh). Nonetheless, the energy mix remained consistent, with PV contributing the majority share in both cases (81.3% vs. 74.4%). This alignment supports the validity of the model under different system scales and conditions.

The relatively high excess electricity in the optimized system is not a result of inefficiency but rather a design choice to ensure uninterrupted power supply in an off-grid context with limited battery storage (2 × 1 MWh). HOMER's algorithm tends to oversize renewable generation (particularly PV) to guarantee that all load is covered year-round, even during periods of low resource availability. During times of low demand or high solar output, this leads to surplus electricity that cannot be stored. However, HOMER penalizes unmet load more heavily than excess energy, making surplus a reasonable trade-off to ensure system reliability. In isolated systems such as this, prioritizing energy security (even at the cost of higher excess) is both technically justified and economically acceptable.

CONCLUSION

Hybrid renewable energy systems offer a practical way to expand energy access in rural agricultural areas. In this research, a hybrid system combining solar panels, wind turbines, biomass generators, and lithium-ion batteries was developed and optimized to supply the energy needs of a poultry and livestock farm in Egypt's New Valley Governorate. The simulation results from HOMER software showed that the PV, wind, biomass, and battery combination was the most economical setup, with a total net present cost of \$9.62 million and a levelized cost of electricity of \$0.716 kWh.

Photovoltaic energy contributed the largest share of electricity generation (82%), supplemented by wind (9.8%) and biomass (8.2%). Sensitivity analyses highlighted the importance of system flexibility and resource availability in achieving optimal performance. Overall, the findings demonstrate the viability of tailored hybrid systems in improving energy reliability and economic sustainability in remote farming communities.

REFERENCES

Alzahrani, A., Hayat, M. A., Khan, A., Hafeez, G., Khan, F. A., Khan, M. I., & Ali, S. (2023). Optimum sizing of stand-alone microgrids: Wind turbine, solar photovoltaic, and energy storage system. *Journal of Energy Storage*, 73, 108611. https://doi.org/10.1016/j.est.2023.108611

Barelli, L., Bidini, G., Bonucci, F., Castellini, L., Fratini, A., Gallorini, F., & Zuccari, A. (2019). Flywheel hybridization to improve battery life in energy storage systems coupled to RES plants. Energy, 173, 937–950. https://doi. org/10. 1016/j. energy.2019.02.143

Das, M., Singh, M. A., & Biswas, A. (2019). Techno-economic optimization of an off-grid hybrid renewable energy system using metaheuristic optimization approaches – Case of a radio transmitter station in India. *Energy Conversion and Management*, 185, 339–352. https://doi.org/10. 1016/j.enc onman.2019.01.107

Das, S., Maitra, S. K., Thrinath, B. S., Choudhury, U., Swathi, G., & Datta, G. (2024). An effective sizing study on PV-wind-battery hybrid renewable energy systems. e-Prime - Advances in Electrical Engineering, Electronics and *Energy*, 10, 100824. https://doi.org/10.1016/j.prime.2024.100824

El-Maaroufi, A., Daoudi, M., & Ahl Laamara, R. (2024). Technoeconomic analysis of a PV/WT/biomass off-grid hybrid power system for rural electrification in northern Morocco using HOMER. Renewable *Energy*, 231, 120904. https://doi.org/10.1016/j.renene.2024.120904

- El-Sattar, H. A., Kamel, S., Hassan, M. H., & Jurado, F. (2022). Optimal sizing of an off-grid hybrid photovoltaic/biomass gasifier/battery system using a quantum model of Runge Kutta algorithm. *Energy Conversion and Management*, 258, 115539. https://doi.org/10.1016/j.enconman.2022.115539
- Emrani, A., & Berrada, A. (2024). A comprehensive review on technoeconomic assessment of hybrid energy storage systems integrated with renewable energy. *Journal of Energy Storage*, 84, 111010. https://doi.org/10.1016/j.est.2024.111010
- Eteiba, M., Barakat, S., Samy, M., & Wahba, W. I. (2018). Optimization of an off-grid PV/Biomass hybrid system with different battery technologies. Sustainable Cities and Society, 40, 713–727. https://doi.org/10.1016/j.scs.2018.01.012
- Guezgouz, M., Jurasz, J., Bekkouche, B., Ma, T., Javed, M. S., & Kies, A. (2019). Optimal hybrid pumped hydro-battery storage scheme for off-grid renewable energy systems. *Energy Conversion and Management*, 199, 112046. https://doi.org/10.1016/j.enconman.2019.112046
- Jahangir, M. H., Moradi, K., & Rashidi, R. (2024). Optimizing and simulating the stand–alone hybrid renewable energy systems for Bandar-E Anzali in Iran. 2024 9th *International Conference on Technology and Energy Management (ICTEM)*, 1–8. https://doi.org/10.1109/ictem60690.2024.10632024
- Kotb, K. M., Elmorshedy, M. F., Salama, H. S., & Dán, A. (2022). Enriching the stability of solar/wind DC microgrids using battery and superconducting magnetic energy storage based fuzzy logic control. *Journal of Energy Storage*, 45, 103751. https://doi.org/10.1016/j.est.2021.103751
- Kumar, P., Pal, N., & Sharma, H. (2022). Optimization and technoeconomic analysis of a solar photovoltaic/biomass/diesel/battery hybrid off-grid power generation system for rural remote electrification in eastern India. *Energy*, 247, 123560. https://doi.org/ 10.10 16/j.energy.2022.123560
- Lin, X., & Lei, Y. (2017). Coordinated control strategies for SMES-battery hybrid energy storage systems. IEEE Access, 5, 23452–23465. https://doi.org/10.1109/access.2017.2761889
- Mahdavi, M., Jurado, F., Ramos, R. A., & Awaafo, A. (2023). Hybrid biomass, solar and wind electricity generation in rural areas of Fez-meknes region in Morocco considering water consumption of animals and anaerobic digester. *Applied Energy*, 343, 121253. https://doi.or/g/10.1016/j.apenergy.2023.121253
- Belrzaeg, M., Abou Sif, M., Almabsout, E., & Benisheikh, U. A. (2023). Distributed generation for Microgrid technology. *International Journal of Scientific Research Updates*, 6(1), 083–092. https://doi.org/10.53430/ijsru.2023.6.1.0062
- Ngila Mulumba, A., & Farzaneh, H. (2023). Techno-economic analysis and dynamic power simulation of a hybrid solarwind-battery-flywheel system for off-grid power supply in remote areas in Kenya. *Energy Conversion and Management:* X, 18, 100381. https://doi.org/10.1016/j.ecmx.2023.100381

- Osmani, A., & Zhang, J. (2014). Optimal grid design and logistic planning for wind and biomass based renewable electricity supply chains under uncertainties. *Energy*, 70, 514–528. https://doi.org/10.1016/j.energy.2014.04.043
- Quizhpe, K., Arévalo, P., Ochoa-Correa, D., & Villa-Ávila, E. (2024).
 Optimizing Microgrid planning for renewable integration in power systems: A comprehensive review. *Electronics*, 13(18), 3620. https://doi.org/10.3390/electronics13183620
- Saxena, A., Aishwarya, B., Badhoutiya, A., Raj, V. H., Gupta, M., & Khayoon, A. T. (2024). Designing a resilient Microgrid for disaster-prone areas using renewable energy sources. 2024 International Conference on Trends in Quantum Computing and Emerging Business Technologies, 1–6. https://doi.org/10.1109/tqcebt59414.2024.10545138
- Siddaraju, C., Deepak, S., & Balasubramanya, H. S. (2022). Optimal design of smart grid renewable energy system using Homer programme. *Journal of Mines, Metals and Fuels*, 70(3A), 134. https://doi.org/10.18311/jmmf/2022/30682
- Dixit, S. (2024). Micro grid integration of distributed power generation optimal operating methods. *Journal of Electrical Systems*, 20(6s), 1043–1050. https://doi.org/10.52783/jes.2836
- Tiam Kapen, P., Medjo Nouadje, B. A., Chegnimonhan, V., Tchuen, G., & Tchinda, R. (2022). Techno-economic feasibility of a PV/battery/fuel cell/electrolyzer/biogas hybrid system for energy and hydrogen production in the far North Region of Cameroon by using HOMER pro. Energy Strategy Reviews, 44, 100988. https://doi.org/10.1016/j.esr.2022.100988
- Won, W., Kwon, H., Han, J., & Kim, J. (2017). Design and operation of renewable energy sources based hydrogen supply system: Technology integration and optimization. *Renewable Energy*, 103, 226–238. https://doi.org/10.1016/j.renene.2016.11.038
- Yadav, S., Kumar, P., & Kumar, A. (2024). Techno-economic assessment of hybrid renewable energy system with multi energy storage system using HOMER. *Energy*, 297, 131231. https://doi.org/10.1016/j.energy.2024.131231
- Youssef, A. A., Barakat, S., Tag-Eldin, E., & Samy, M. (2023). Islanded green energy system optimal analysis using PV, wind, biomass, and battery resources with various economic criteria. Results in Engineering, 19, 101321. https://doi.org/10.1016/j.rineng.2023.101321
- Zhang, W., Maleki, A., Rosen, M. A., & Liu, J. (2019). Sizing a standalone solar-wind-hydrogen energy system using weather forecasting and a hybrid search optimization algorithm. *Energy Conversion and Management*, 180, 609–621. https://doi.org/10.1016/j.enconman.2018.08.102

تحسين وتحليل الحساسية لمنظومات هجينة مستقلة من الطاقة الشمسية وطاقة الرياح والكتلة الحيوية والبطاريات لكهربة زراعية مستدامة في المناطق النائية

أحمد جادو ، تتيانا موروزوق و جينمينج بان "

- · قسم الهندسة الزراعية والنظم الحيوية كلية الزراعة جامعة المنصورة مصر
 - ٢ معهد هندسة الطاقة جامعة براين التقنية براين ألمانيا
 - ^r قسم هندسة النظم الحيوية جامعة تشجيانغ هانغتشو الصين

الملخص

نتناول هذه الدراسة تقييم الجنوى التقنية والاقتصادية لأنظمة الطاقة المتجددة الهجينة بهدف تلبية احتياجات الكهرباء لمزرعة لتربية الماشية والدواجن في محافظة الوادي الجديد بجمهورية مصر العربية. تم استخدام برنامج HOMER Pro لمحاكاة عدة تكوينات لأنظمة الطاقة، تجمع بين الخلايا الشمسية الكهر وضوئية وتوربينك الرياح والمولدات العاملة بالكتلة الحيوية وأنظمة تخزين البطاريات، ونلك استنادًا إلى بيانات مناخية محلية تفصيلية ونماذج جمل كهربائي حقيقية على مدار الساعة. أظهرت النتائج أن نظام الطقة الشمسية/الرياح/الكتلة الحيوية/البطاريات كان الخيل الأكثر كفاءة من حيث التكلفة، حيث حقق تكلفة حالية صافية قرها ٩٠٦٢ مليون دو لار أمريكي وكلفة طاقة مستوية تبلغ ٢١٦,٠ دو لار أمريكي لكل كيلوواطم ساعة. وفرت الطاقة الشمسية معظم احتياجات المررعة من الكهرباء، بينما ساهمت طاقة الرياح والكتلة الحيوية بنسبة أقل ولكنها مهمة. كشفت تحليلات الحساسية أن التحسينات الطفيفة، مثل خفض التكليف الرأسمالية أو تحسين توفر مصادر الطاقة المتجددة، يمكن أن تجعل هذه الأنظمة أكثر جدوى اقتصاديًا. تؤكد النتائج أن الدمج المدروس لمصادر الطاقة المتجددة بمكن أن تجعل هذه الأنظمة أكثر جدوى اقتصاديًا. تؤكد النتائج أن الدمج المدروس لمصادر الطاقة في المناطق الزراعية النائية.